Communication: Dynamical embedding: Correct quantum response from coupling TDDFT for a small cluster with classical near-field electrodynamics for an extended region

Yi Gao and Daniel Neuhauser

Department of Chemistry and Biochemistry, University of California, Los Angeles, California 90095-1569, USA

We show how to obtain the correct electronic response of a large system by embedding; a small region is propagated by TDDFT (time-dependent density functional theory) simultaneously with a classical electrodynamics evolution using the Near-Field method over a larger external region. The propagations are coupled through a combined time-dependent density yielding a common Coulomb potential. We show that the embedding correctly describes the plasmonic response of a Mg(0001) slab and its influence on the dynamical charge transfer between an adsorbed H_2O molecule and the substrate, giving the same spectral shape as full TDDFT (similar plasmon peak and molecular-dependent differential spectra) with much less computational effort. The results demonstrate that atomistic embedding electrodynamics is promising for nanoplasmonics and nanopolaritonics. © *2013 AIP Publishing LLC.* [http://dx.doi.org/10.1063/1.4804544]

Molecular plasmonics (a.k.a. nanopolaritonics),[1–4] a new field investigating the interaction between molecules and surface plasmons, requires modeling of a large number of electrons coupled to an electromagnetic field. Time dependent density functional theory (TDDFT) has been widely used to study quantum effects in plasmonics[5–7] that are missing in conventional classical electrodynamics models.[8–10] However, TDDFT is expensive so a multiscale approach bridging the molecular and plasmonic scales is needed.[11–13]

Recently, we developed an embedding electrodynamics approach.[14] (For other approaches see Refs. 15–20) Our approach describes nanostructures as quantum systems embedded within a frequency-dependent dielectric medium; the systems are propagated simultaneously, coupled through an overall time-dependent potential. The method was demonstrated on a one-dimensional jellium system.

Here we extend the quantum embedding method, with the new feature of explicit inclusion of molecular orbitals that are expanded with atomic basis sets. The electrodynamics of the entire system is calculated by propagating each subsystem (TDDFT for the quantum part and near-field (NF)[10] for the classical part) simultaneously and the common Coulomb potential is evaluated and used at each step. We demonstrate that the resulting atomistic embedding method is successful at mimicking full scale TDDFT for describing the plasmonic response of a Mg slab and the dynamical charge transfer (CT) between an adsorbed H_2O molecule and substrate. Thus, the work demonstrates that embedding is useful even for chemically covalent systems (metal-molecule here) and that a small quantum region is sufficient for realistic simulation of the molecular response, with the classical NF part ensuring that there are no energy reflection effects from the edges of the quantum region. The resulting embedding methodology is not restricted to TDDFT/NF and is appropriate for more elaborate quantum theories.

The key in the embedding is that both the embedded quantum system and the classical environment are subjected to the same electric potential ϕ, obtained from the time-dependent combined quantum+classical density through a time-dependent Poisson equation (using $e = \hbar = m_e = 1$),

$$
\begin{aligned}
-\epsilon_0 &\nabla \cdot (\epsilon(\mathbf{r}) \nabla \phi(\mathbf{r}, t)) \\
&= n(\mathbf{r}, t) - n_{\mathrm{ion}}(\mathbf{r}) + \rho_{\mathrm{NF}}(\mathbf{r}, t) \\
&\quad + \epsilon_0 \nabla^2 (\delta\phi_{\mathrm{ext}}(\mathbf{r}, t)),
\end{aligned}
\tag{1}
$$

where we introduced the classical static dielectric constant of the background $\epsilon(\mathbf{r})$, the quantum electron density n, the ionic background n_{ion}, the NF electron density ρ_{NF}, and the external potential $\delta\phi_{\mathrm{ext}}$. This equation is general and as explained below the dynamic response of the background is accounted for in $\rho_{\mathrm{NF}}(\mathbf{r}, t)$.

Once it is accepted that the same electric potential governs both the quantum and classical systems, the rest of the formalism is straightforward. The quantum electron density, $n(\mathbf{r}, t) = 2 \sum_i^{\mathrm{occ}} |\psi_i(\mathbf{r}, t)|^2$, is obtained by propagating the time-dependent Kohn-Sham (TD-KS) equation

$$
\begin{aligned}
i \frac{\partial \psi_i(\mathbf{r}, t)}{\partial t} &= \hat{h} \psi_i(\mathbf{r}, t) \\
&= \left(-\frac{1}{2}\nabla^2 + \phi(\mathbf{r}, t) + \delta\phi_{\mathrm{ext}}(\mathbf{r}, t) \right. \\
&\quad \left. + \upsilon_{\mathrm{xc}}(\mathbf{r}, t) \right) \psi_i(\mathbf{r}, t),
\end{aligned}
\tag{2}
$$

where we introduced the time-dependent single-particle Hamiltonian operator $\hat{h}$ and the exchange correlation (xc) potential υ_{xc}. Note that the ion-electron interaction is included in the overall NF potential ϕ, determined through Eq. (1).

The classical background is described by the NF method, where the main ingredient is the NF density. (This facilitates

138, 181105-1

the embedding since the NF and TDDFT densities combine straightforwardly.) The NF density is obtained from a sum of a small number (labeled N_j, typically 1–9) of Drude-Lorentz classical polarizations, $\rho_{NF}(\mathbf{r}, t) = -\nabla \cdot \sum_{j=1}^{N_j} \mathbf{P}_j$ fulfilling

$$\frac{d^2}{dt^2}\mathbf{P}_j(\mathbf{r}, t) = -\alpha_j(\mathbf{r})\frac{d}{dt}\mathbf{P}_j(\mathbf{r}, t) - \bar{\omega}_j^2(\mathbf{r})\mathbf{P}_j(\mathbf{r}, t)$$
$$+ \epsilon_0\beta_j(\mathbf{r})\mathbf{E}(\mathbf{r}, t), \qquad (3)$$

where the Drude-Lorentz coefficients are obtained by fitting the frequency dependent dielectric response. The Drude-Lorentz fit is used for the same reason that it is popular in full scale Maxwell studies, i.e., it enables the representation of a delayed frequency-dependent response through an instantaneous time-dependent propagation. The electric field is assumed longitudinal

$$\mathbf{E}(\mathbf{r}, t) = -\nabla\phi(\mathbf{r}, t) - \nabla\delta\phi_{ext}(\mathbf{r}, t). \qquad (4)$$

Numerically, the time-dependent equations (Eqs. (2) and (3)) are propagated simultaneously, maintaining self-consistency between the classical NF fields and quantum TD-KS orbitals. In practice, the TD-KS equations are represented by atomic basis sets; in this work the density matrix $\mathbf{D}$ (rather than individual orbitals) is propagated as usual,

$$\mathbf{D}(t + \Delta t) = \mathbf{U}(t + \Delta t, t)\mathbf{D}(t)\mathbf{U}^\dagger(t + \Delta t, t), \qquad (5)$$

and a Magnus expansion is used for $\mathbf{U}$,

$$\mathbf{U}(t + \Delta t, t) = \exp\left(-i\Delta t\mathbf{S}^{-1}\mathbf{h}\left(t + \frac{\Delta t}{2}\right)\right), \qquad (6)$$

where we introduced the atomic orbital overlap and single-particle matrices, $\mathbf{S}$ and $\mathbf{h}$. Simultaneously, the NF polarizations are propagated using a simple leap-frog algorithm that discretizes Eq. (3), see Ref. 10 for details.

The initial conditions for the propagation are that before the excitation the potential $\phi_0 = \phi(t = 0)$ does not vary in time, so that the static KS orbitals, $\psi_{i,0}$'s, fulfill

$$\left(-\frac{1}{2}\nabla^2 + \phi_0(\mathbf{r}) + \upsilon_{xc}(\mathbf{r})\right)\psi_{i,0}(\mathbf{r}) = \epsilon_i\psi_{i,0}(\mathbf{r}), \qquad (7)$$

simultaneously with the overall static Poisson equation, which becomes

$$-\epsilon_0\nabla^2\phi_0(\mathbf{r}) = n_0(\mathbf{r}) - n_{ion}(\mathbf{r})$$
$$+ (\epsilon(\mathbf{r}, 0) - \epsilon_0)\nabla\phi_0(\mathbf{r}). \qquad (8)$$

After convergence, the static NF density and TDDFT orbitals are subjected to a delta-function pulse $\phi_{ext}(\mathbf{r})\delta(t)$ and Eqs. (2) and (3) are propagated forward in time.

We apply the atomistic embedding electrodynamics to study the plasmonic response of a Mg(0001) slab and its influence on the CT between an adsorbed H_2O molecule and a Mg substrate. (All nuclei are frozen here, though the method is equally applicable when the nuclei move; in the classical region, the jellium response should then be taken as experimental, including nuclear polarization effects.) Mg is an ideal initial substrate, as its electronic structure description is simple (unlike transition metals such as gold or silver), it possesses a well-defined plasmon and conjugates well to simple molecules. Unlike gold or silver, however, the plasmon is
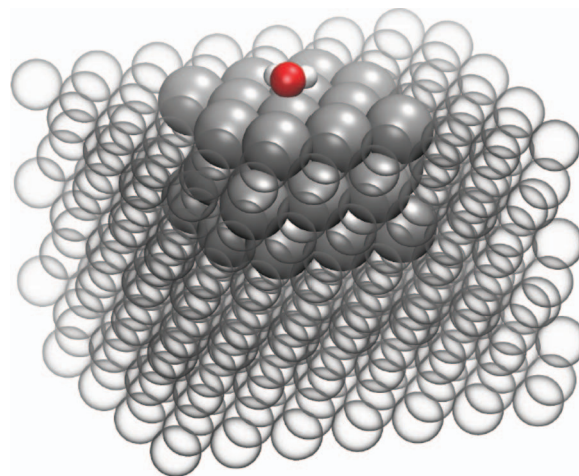
FIG. 1. Embedding a Mg(0001) slab. The entire 6-layer Mg slab is partitioned as a 3-layer 3×4 Mg cluster with 36 atoms (solid gray spheres) of size $9.6 \times 11.1 \times 7.8$ Å^3 embedded within a near-field (NF) metal (transparent part). The Mg cluster is the central upper part of the entire slab. The adsorption geometry of a H_2O molecule (red and white spheres) is also displayed.

in the UV ($\sim 9 - 10$ eV) so we used water as the adsorbed molecule as it has a strong absorption feature around that energy.

The embedding strategy is illustrated in Fig. 1. We implemented the method in the SIESTA package,[21] using norm-conserving pseudopotentials,[22] double-zeta plus polarization basis sets, and the generalized gradient approximation functional with Perdew-Burke-Ernzerhof parameterization (GGA-PBE) functional.[23] Periodic boundary condition was used for infinite slab. Further, a single k-point sampling is used, which is reasonable because of the size of the system (we verified that the important feature, the DOS (density of states) is almost the same for many- and single-point sampling). The dielectric function of the Mg metal is fitted to a full-scale TDDFT calculation with a single Drude-Lorentz oscillator with parameters $\alpha_1 = 0.5$ eV, $\beta_1 = 10.89^2$ eV^2, and $\bar{\omega}_1 = 0.32$ eV; the fit is excellent in the relevant frequency range ($2-16$ eV), as seen in Fig. 2. All quantum/classical interfaces were chosen between adjacent atomic planes and the NF electron density (i.e., $\beta(\mathbf{r})$) falls off smoothly (over 0.8 Å) to reduce discontinuities. We study the linear response of system to an electric delta-function (in time) pulse with polarization normal to the surface. All propagations use a uniform $\Delta t = 0.5$ a.u. for 2000 steps.

First, a clean slab (no H_2O) is studied. The dynamical response of the Mg(0001) slab is given by the normalized average dipole moment, $\bar{d}(t) = \frac{\mathbf{n}\cdot\mathbf{d}(t)}{|E_0|N_a}$ (N_a is the total number of atoms, $\mathbf{n}$ is the unit surface normal, and $\mathbf{d}$ is the total dipole). The corresponding average polarizability is $\bar{\alpha}(\omega) = \int dt\, e^{i\omega t - \eta t}\bar{d}(t)$, where $\eta = 0.15$ eV is used for broadening.

The calculated dipoles using different methods are compared in Fig. 2(a). All results decay initially due to band-structure induced damping.[24] The full-scale TDDFT calculation for the entire slab serves as a benchmark and is used to fit the parameters in the NF calculations. However, the uniform decay in the NF result is more physical since both the finite k-sampling and adiabaticity of the xc potential
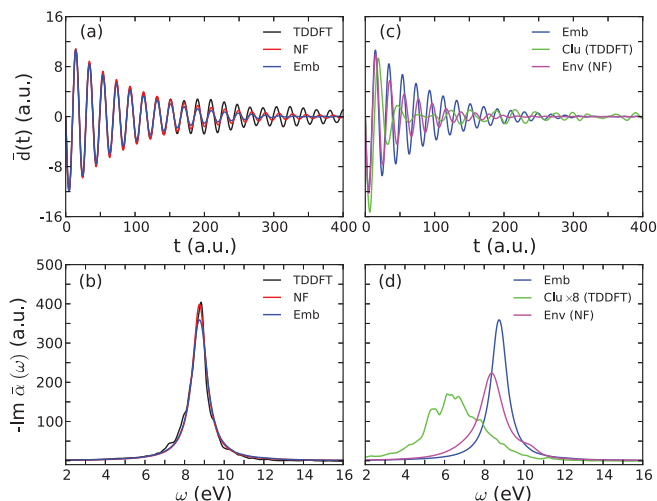
FIG. 2. (a) Normalized average dipoles and (b) absorption coefficients (imaginary part of the polarizabilities) for a clean Mg slab calculated by different methods: fully TDDFT (all quantum), NF (classical), and embedding. In (c) and (d) the embedding result is compared with dipoles and absorption of a free cluster (clu-TDDFT) and a bare dielectric environment (env-NF).

FIG. 3. (a) Differential polarizability between adsorbed and clean Mg surface and (b) dynamical charge transfer to the H_2O by the different methods: full TDDFT of the entire system (339 atoms), an isolated small cluster of the embedded H_2O molecule with 36 Mg atoms, which does not agree with the TDDFT results; and embedding quantum mechanical clusters with 36 and 90 ("big") Mg atoms; the TDDFT and both embedded clusters show an overall shoulder between 7 and 8.5 eV (with better agreement for the larger cluster), while the free cluster is strongly shifted to lower frequencies.

underestimate the plasmonic damping in TDDFT.[25] The embedding dipole agrees well with both other methods till 200 a.u. and continues to track the NF result with a good phase agreement up to 300 a.u.

The success of embedding is also demonstrated in the frequency-domain absorption (Fig. 2(b)), where all responses are similar. Figures 2(c) and 2(d) prove that embedding is necessary, since a small non-embedded cluster shows dipole-moment oscillations characteristic of reflection. Therefore, the atomistic embedding is necessary—the embedding facilitates the transport of the time dependent electric signal from the quantum to the classical region without reflections.

We next focus on the effect of a H_2O molecule adsorption on the plasmon resonance and the CT between the molecule and the Mg(0001) slab. The molecule lies flat on the surface and the O atom is right on top of a surface Mg atom with a distance of 2.4 Å. This structure mimics many experiments studying plasmonics and polaritonics. The GGA functional is limited for CT, but our main goal is to demonstrate that embedding enables the use of a small cluster, so the accuracy of the details of the functional, which will mainly affect the molecular CT, is less relevant; future studies will incorporate long-range functionals for CT.

Figure 3(a) shows the differential absorption coefficient, i.e., the change of the imaginary part of polarizability before and after molecular adsorption. The full TDDFT calculation shows that the absorption near the plasmon resonance around 8.7 eV is reduced when a molecule is added. This is due to energy transfer from the metal to the molecule. Without the dielectric environment, the cluster+H_2O result fails to describe this behavior, but when the NF environment is embedded, the dip is reproduced.

To further study the effects of the H_2O adsorption, we show in Fig. 3(b) the imaginary part of the frequency-dependent Mulliken charge transfer on the molecule ($\Delta \bar{Q}(\omega) = \frac{1}{|E_0|} \int dt \, e^{i\omega t - \eta t} \Delta Q(t)$, where $\Delta Q(t)$ is the charge transferred to the molecule) as it is an indication of the in-

volvement of CT in the plasmonic absorption. Again, embedding reproduces the TDDFT charge transfer, whereas a free cluster+molecule model is qualitatively different. For embedding with a 36 atom cluster $\Delta \bar{Q}(\omega)$ shows a peak at $\sim$5.5 eV (also manifested as a small feature in the differential absorption) due to residual interaction between the cluster edge and the molecule, which disappears when a larger embedded cluster is used (a three layer 5 × 6 cube, with 90 Mg atoms). For the bigger cluster, the spectral shape of the CT oscillation has a shoulder at $\sim$7 eV, in good agreement with full TDDFT.

The new embedding method is much cheaper than all-TDDFT simulations since the expensive TDDFT part is only performed for a small cluster; for example, the 36 atom simulation was 12 times faster than a full 339 atom TDDFT study, while the 90 atoms cluster took 5 times less than the full study. Furthermore, the savings will be much larger for bigger systems where the TDDFT effort scales as the square or cube of the system size, depending on the implementation.

Finally, our embedding method is not restricted to TDDFT and NF electrodynamics: for example, for the quantum subsystem, advanced theories, such as a TD optimized effective potential[26] or even TD correlated wavefunction methods,[27] can be directly employed; these advanced theories will be used in the future for describing CT and Raman processes in nanoplasmonics.

[1] R. P. Van Duyne, Science **306**, 985 (2004).
[2] D. Neuhauser and K. Lopata, J. Chem. Phys. **127**, 154715 (2007).
[3] A. J. White, M. Sukharev, and M. Galperin, Phys. Rev. B **86**, 205324 (2012).
[4] A. O. Govorov and Z. Fan, ChemPhysChem **13**, 2551 (2012).
[5] J. Zuloaga, E. Prodan, and P. Nordlander, Nano Lett. **9**, 887 (2009).
[6] P. Song, P. Nordlander, and S. Gao, J. Chem. Phys. **134**, 074701 (2011).
[7] S. M. Morton, D. W. Silverstein, and L. Jensen, Chem. Rev. **111**, 3962 (2011).
[8] A. Taflove, *Advances in Computational Electrodynamics: The Finite-Difference Time-Domain Method* (Artech House, Boston, 1998).
[9] E. Prodan, C. Radloff, N. J. Halas, and P. Nordlander, Science **302**, 419 (2003).
[10] A. Coomar, C. Arntsen, K. A. Lopata, S. Pistinner, and D. Neuhauser, J. Chem. Phys. **135**, 084121 (2011).
[11] D. J. Masiello and G. C. Schatz, Phys. Rev. A **78**, 042505 (2008).
[12] J. L. Payton, S. M. Morton, J. E. Moore, and L. Jensen, J. Chem. Phys. **136**, 214103 (2012).
[13] R. Esteban, A. G. Borisov, P. Nordlander, and J. Aizpurua, Nat. Commun. **3**, 825 (2012).
[14] Y. Gao and D. Neuhauser, J. Chem. Phys. **137**, 074113 (2012).
[15] N. Govind, Y. A. Wang, and E. A. Carter, J. Chem. Phys. **110**, 7677 (1999).
[16] J. D. Goodpaster, N. Ananth, F. R. Manby, and T. F. Miller III, J. Chem. Phys. **133**, 084103 (2010).
[17] C. Huang, M. Pavone, and E. A. Carter, J. Chem. Phys. **134**, 154110 (2011).
[18] A. Liebsch, *Electronic Excitations at Metal Surfaces* (Plenum Press, New York, 1997).
[19] J. M. Lastra, J. W. Kaminski, and T. A. Wesolowski, J. Chem. Phys. **129**, 074107 (2008).
[20] W. Liang, X. Li, L. R. Dalton, B. H. Robinson, and B. E. Eichinger, J. Phys. Chem. B **115**, 12566 (2011).
[21] J. M. Soler, E. Artacho, J. D. Gale, A. Garcia, J. Junquera, P. Ordejon, and D. Sanchez-Portal, J. Phys.: Condens. Matter **14**, 2745 (2002).
[22] N. Troullier and J. L. Martins, Phys. Rev. B **43**, 1993 (1991).
[23] J. P. Perdew, K. Burke, and M. Ernzerhof, Phys. Rev. Lett. **77**, 3865 (1996).
[24] V. M. Silkin, E. V. Chulkov, and P. M. Echenique, Phys. Rev. Lett. **93**, 176801 (2004).
[25] W. Ku and A. G. Eguiluz, Phys. Rev. Lett. **82**, 2350 (1999).
[26] C. A. Ullrich, U. J. Gossmann, and E. K. Gross, Phys. Rev. Lett. **74**, 872 (1995).
[27] M. R. Silva-Junior, M. Schreiber, S. P. Sauer, and W. Thiel, J. Chem. Phys. **129**, 104103 (2008).